

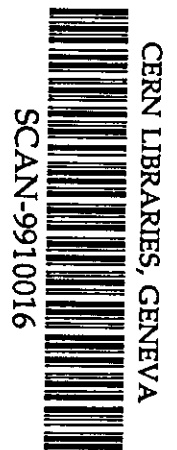
DD γ



Technical Report
RAL-TR-1999-057

Studies of the Gain Properties of Gas Microstrip Detectors Relevant to Their Application as X-Ray and Electron Detectors

J E Bateman J F Connolly G E Derbyshire D M Duxbury J Lipp
J A Mir R Stephenson J E Simmons and E J Spill



13th August 1999

© Council for the Central Laboratory of the Research Councils 1999

Enquiries about copyright, reproduction and requests for additional copies of this report should be addressed to:

The Central Laboratory of the Research Councils
Library and Information Services
Rutherford Appleton Laboratory
Chilton
Didcot
Oxfordshire
OX11 0QX
Tel: 01235 445384 Fax: 01235 446403
E-mail library@rl.ac.uk

ISSN 1358-6254

Neither the Council nor the Laboratory accept any responsibility for loss or damage arising from the use of information contained in any of their reports or in any communication about their tests or investigations.

**STUDIES OF THE GAIN PROPERTIES OF GAS MICROSTRIP
DETECTORS RELEVANT TO THEIR APPLICATION AS
X-RAY AND ELECTRON DETECTORS**

J E Bateman, J F Connolly, G E Derbyshire, D M Duxbury, J Lipp, J A Mir,
R Stephenson, J E Simmons and E J Spill

Rutherford Appleton Laboratory, Chilton, Didcot, Oxon, OX11 0QX, UK

Abstract

Because both the anodic and cathodic gain-defining elements are produced lithographically on the same rigid substrate, the Gas Microstrip Detector (GMSD) makes an excellent planar (position sensitive) amplifier of incident electron clouds. We have studied the dependence of the gas gain and pulse height resolution of the plate as a function of various geometric and gas parameters. The results show that a GMSD can be made very insensitive to the shape of the drift electrode, allowing it to be used in a wide variety of applications. An example of an electron-yield X-ray Absorption Fine Structure (XAFS) study is given.

1. Introduction

The present proliferation of Synchrotron Radiation Sources capable of producing extremely intense beams of x-rays leads to an ongoing search for x-ray detecting systems capable of exploiting the potential high photon statistics in typical materials studies such as X-ray Absorption Fine Structure (XAFS) and small (and large) angle scattering. There is a natural preference that such detectors should (if possible) be counting systems which can (in principle) be limited in resolution only by the counting statistics. Attention has turned to the classic gas-filled wire proportional counter which is, however, severely limited in its rate capability and working geometry. A form of gas proportional counter which has much more attractive properties for these demanding applications is the Gas Microstrip Detector (GMSD).

In the GMSD the electrode pattern of the gas amplifying structure is realised on a plate of some suitable semi-insulating material using microlithography techniques. Fine anode strips (typically 10 μ m wide) are interleaved with cathode strips (typically >100 μ m wide) in a repetitive pattern which (typically) has a period of several hundred microns. When a potential of about ≈ 700 V is established between anode and cathode strips in a suitable gas atmosphere free electrons experience amplification near the anodes. These signals can be detected on individual anodes or on areas of bussed anode strips. Introduced by Oed [1] and subjected to a decade of continuous development for particle tracking applications in the demanding environment of the next generation of Particle Physics collider experiments [2-7] the GMSD has been demonstrated to possess rate and lifetime capabilities never previously seen in gas-filled counters. In particular, operation has been demonstrated at rate densities of up to 1MHz/mm² of plate [8] and useful lifetimes corresponding to several months of continuous running at these rates [9].

Apart from the problem of operating at high rates the demands of x-ray detection are rather different from those of trackers in Particle Physics. In particular gain stability and pulse height resolution are important, as is the ability to maintain all essential properties in a detector which can be contained within a volume of a few tens of cubic centimeters and operated within millimeters of the sample. Very high counting rates rapidly break down the quencher component of the counter gas so that flowing gas is essential. The use of flowing gas leads to questions of gain stability against variations in ambient conditions and gas composition which do not arise with sealed counters.

An interesting possibility opened up by the use of the GMSD is the option to detect the auger electrons released from a sample surface by the x-rays of the SRS beam. The sample can form part of the structure of the counter so that experiments can be conducted at ambient conditions in the counter gas, in the composition of which one has a degree of flexibility as long as strongly electronegative gases (such as oxygen) are avoided. The usefulness of this approach depends partly on a flowing gas system which will allow samples to be changed and the counter operating again within a short (e.g. <1 hour) period.

In this paper we report the results of detailed studies of the effect of different design and operational parameters on the gain of the GMSD and show that stable and flexible

operation is possible with GMSDs in the experimental configurations necessary for high rate operation on SRS experiments.

2. Equipment

The basic design of a GMSD is extremely simple. As figure 1 shows, it consists of the plate with the metallised electrode pattern supported at a suitable distance (anything from 1mm to several centimeters) from a drift cathode which defines the interaction volume in which the x-rays (or electrons) can convert into slow electrons. The latter drift down onto the nearest anode strips and are multiplied by factors of >1000 . The lithographic strip pattern of $300\mu\text{m}$ period, $90\mu\text{m}$ wide anodes and a range of anode widths varying from $2\mu\text{m}$ to $10\mu\text{m}$ was laid down on Schott S8900 semi-insulating glass in a process which plated $0.5\mu\text{m}$ of gold on to of a thin nickel substrate. This work was carried out by our collaborators at VTT Electronics in Espoo, Finland. The strips are bussed into groups of twenty with the anode and cathode connections collected in large pads at each end and to which simple pressure connections are made. The active area of each section is 12mm (along the strips) and 6mm across. There are seven such sections (each independently connected) on a glass plate measuring 50mm square. Within each section the anode width is constant but it is varied between sections within the range $2\mu\text{m}$ to $5\mu\text{m}$. A separate plate (of otherwise identical design) is used for the data on $10\mu\text{m}$ anodes.

The drift electrode and cathodes are operated negative with respect to the anodes which are held close to earth and connected to a standard Ortec pulse height analysis chain with $1\mu\text{s}$ shaping time constants in the main amplifier which in turn feeds a pulse height analyser. Gain calibration is arranged by means of an Ortec precision pulser which supplies a known test charge to the preamplifier input (2% absolute calibration error). The mean energy per ion pair for the argon-isobutane mixtures used is taken as 28eV and no allowance is made for the small changes (a few %) which occur in this parameter as the relative fractions change. (In general use the gas mixture is held fixed.)

The gas mixture is controlled by Brooks mass-flow controllers (model 5850E) built into a rig fabricated in stainless steel tubing which is used throughout with the exception (occasionally) of small sections of flexible plastic tubing close to the detector to facilitate mounting. The absolute accuracy of the gas mixing is given as 1% with a repeatability of 0.25% of the flow.

In the tests described an x-ray source of Mn x-rays (^{55}Fe) at 5.9keV illuminates the detector drift space parallel to the plate through a melinex foil window in the end wall of the detector box. The x-ray beam passes over the seven sections in turn and allows comparative gain studies with different anodes to be made with the same gas mixture and ambient conditions.

The ambient pressure and the temperature of the detector box are recorded with every measurement.

3. Basic Gain Studies

At first sight the problem of providing a meaningful parameterisation of the gain of a GMSD is a daunting prospect. First one must solve Laplace's equation to get the electric field in the region of the anode (see reference [10]) and integrate the Townsend coefficient along the drift paths of the electrons approaching the anode. Further, this field is controlled by two independently variable potentials on the cathode (V_c) and the drift cathode (V_d). The three terminal problem can be tackled by noting that *provided* the electron cloud representing the x-ray event drifts into the anode *along the same path and without loss*, the gain will be controlled by the resultant electric field in the region above the anode which is just a linear combination of the fields generated by any nearby electrodes. It turns out that in a wide range of operating conditions these necessary conditions hold.

Figure 2 shows a plot of the V_c against V_d when the gain is held constant (i.e. the x-ray peak on the PHA is held at a constant position by decreasing V_c as V_d is raised. An excellent straight line results showing that an effective cathode potential can be defined:

$$V = V_c + \alpha V_d \quad (1)$$

where α is a small number. In figure (1) $\alpha = 0.7\%$ illustrating immediately the weak dependence of the gain of the GMSD on the drift electrode potential since a change of 1000V in V_d will only produce a gain shift equivalent to a shift of 7V in V_c .

Ideally α is independent of the gas mixture. However, substantial changes in the gas mixture can invalidate the two pre-requisite conditions noted above. If the gas is strongly electronegative the carriers are lost and the graph curves upward at low V_d . However, usually a sufficient portion of straight line persists at high V_d to permit reliable evaluation of α . The other condition (constant drift paths) is affected by the diffusion coefficient of the electrons in the gas. At low quencher fractions in a noble gas the diffusion coefficient grows rapidly and the measured value of α rises with it. However, within the general working range of quencher mixtures (10% to 30%) the conditions are met well enough to give linear plots such as figure (1) with approximately constant values of α .

In a previous study it was shown that there is a semi-empirical relation which describes with great accuracy the gain characteristics of a wide range of gas counters in the general range of ambient conditions [11]:

$$\ln M = \frac{V}{A} e^{-\frac{B}{V}} \quad (2)$$

where M is the gas gain, V is the anode-cathode potential difference and A and B are constants which depend on the field geometry, the ambient variables pressure (P) and temperature (T) and the atomic properties of the gas mixture (ionisation cross-sections etc.).

Figure 3 shows a series of gain curves plotted for a section of plate with 10 μ m anodes and varying fractions of isobutane quencher in the gas mixture. The abscissa of the

gain plots is the effective potential defined in equation (1) above. Fits of the form of equation (2) are seen to be universally excellent and the values of A and B are now available to characterise the dependence of the gain on the gas mixture.

The parameterisation permitted by combining equations (1) and (2) makes possible the description of the gain of a GMSD in respect of the essential design and operational parameters as is shown below.

4. Gain Dependence on Strip Geometry

It has been shown elsewhere [12] that the parameters A and B in equation (2) can be modelled on the version of the formula which can be derived explicitly for the case of a single wire, cylindrical proportional counter. As long as the anode-cathode gap is greater than about 20% of the strip period we can approximate as follows:

$$A = p \left\{ \ln \frac{b}{a} \right\}^c$$

$$B = \frac{a}{q} \left\{ \ln \frac{b}{a} \right\}^c$$
(3)

where a is half the width of the anode strip and b the anode-cathode gap. The parameters p , q and include the non-geometric terms in the single wire formula and c is a fitted parameter which takes account of the divergence of the electric field from radial symmetry. This modification of equation (2) was shown to fit well to experimental data for plate patterns with anode widths of $10\mu\text{m}$ and above and for anode cathode gaps limited as noted above [12]. A prediction of the formula was that the gain would peak at anode widths near $5\mu\text{m}$ and decrease at lower anode widths. The present plate permits exploration of this region and figure 4 shows the results of the measurement of the gain as a function of anode width at a constant bias potential along with the fit derived from equations (2) and (3).

Also plotted in figure 4 is the maximum stable operating gain obtainable with each anode width in the given gas mixture. It is interesting to note that it follows the same general trend as the gain at fixed bias. This is in contrast to the situation if the anode-cathode gap is increased when the maximum gain rises as the gain at fixed potential decreases [13].

The turn-over of the gain curve is seen in the data and perhaps the most interesting fact to emerge is that between anode widths of $2\mu\text{m}$ and $5\mu\text{m}$ the dependence of the gain on anode width is very weak with a total change of only -6.6% . This eases constraints on the quality required of the lithography in this region where the lithographic errors begin to become noticeable in percentage terms. (SEM Measurements of a $4\mu\text{m}$ wide anode strip along its length produced an RMS variation of 3.2% .)

5. Gain Dependence on the Drift Gap Width

The drift gap is the “working space” of the GMSD and it is important to have maximum flexibility in adapting it to the various applications that are proposed. In order to study the effect of the drift gap the α parameter was studied as a function of the drift gap width (by raising and lowering it) and also of the anode width. Figure 5 shows α measured as a function of $1/D$ (where D is the drift gap width) for the sections with different anode widths. Unsurprisingly, α is inversely proportional to D and is approximately proportional to the anode width. Figure 6 shows α as a function of the strip width at a constant $D = 11\text{mm}$.

This data can be analysed to produce a general expression for the value of α in this gas mixture (argon + 25% isobutane):

$$\alpha = \left(\frac{0.234w + 5.4}{D} \right) + 0.051\% \quad (4)$$

where w is the anode width in μm .

Combining equation (4) with equations (1) and (2) now yields a complete functional description of the gain of the MSGD as a function of D , w , V_d and V_c . Figure 7 shows the resulting plots for fixed $V(=V_c + \alpha V_d)$ of 630V and variable D for two different anode widths, w . Differentiating the curves in figure 7 shows that $1/M \text{d}M/\text{d}V$ varies from $-0.127/\text{mm}$ at $D = 4\text{mm}$ to $-0.007/\text{mm}$ at $D = 16\text{mm}$ for the $w = 2\mu\text{m}$ curve (the corresponding values for the $w = 5\mu\text{m}$ curve are $-0.131/\text{mm}$ and $-0.008/\text{mm}$).

These numbers illustrate one of the most useful features of the GMSD, namely the possibility of making the gain almost completely independent of the drift cathode position. Provided that $D > 10\text{mm}$ the gain of the counter will only shift by about 2% for a 1mm variation in D . Since the best pulse height resolution obtainable at an x-ray energy of 5.9keV is around 14.5%, this gives one great flexibility for installing sample holders (for electron work) and window fittings (for x-ray work).

6. Gain Dependence on the Gas Mixture

The data of figure 3 contain the information required to derive the dependence of this counter (10 μm anodes) on the gas mixture. The parameter used for the analysis is the percentage of isobutane in the mixture. Differentiating equation (2) with respect to A and B one can obtain the differential gain shift from:

$$\delta M = \frac{dM}{dA} \delta A + \frac{dM}{dB} \delta B$$

which evaluates to:

$$\delta M = -\ln(M) \left\{ \frac{\delta A}{A} + \frac{\delta B}{V} \right\}$$

Substituting $\delta A = \frac{dA}{dx} \delta x$ and $\delta B = \frac{dB}{dx} \delta x$ and expressing as derivatives gives:

$$\frac{1}{M} \frac{dM}{dx} = -\ln M \left\{ \frac{1}{A} \frac{dA}{dx} + \frac{1}{V} \frac{dB}{dx} \right\} \quad (5)$$

where x is the fraction of isobutane in the gas mixture (by volume) and dA/dx and dB/dx are evaluated from a graph of the parameters A and B derived from the fits to equation (2) in figure 3.

Figure 8 shows the relative gain sensitivity (as defined in (5) above) of the GMSD with $10\mu\text{m}$ anodes as a function of the isobutane concentration at a gain of $M = 1000$. Equation (5) can obviously be used to evaluate the relative gain sensitivity as a function of M as well as x . However, it can be shown that under most circumstances the second term in the brackets of (5) dominates and since $V \approx \ln(M)$ the overall gain dependence is very weak.

In the standard operating mixture (argon + 25% isobutane) $1/M dM/dx$ is -0.095 . Assuming that the error in the larger gas fraction dominates the repeatability error in x given for the Brooks mass-flow controller is $0.75 \times 0.25\% = 0.19\%$ which yields a $\delta M/M$ of 0.018 , i.e. 1.8% . This error is comfortably small compared with the typical pulse height resolution ($>14.5\%$ FWHM). In practice one is concerned with the stability of the gas mixture over periods of a few minutes to a few hours during experimental exposures. From experience there is reason to believe that the short term stability of the gas flow is rather better than the 0.25% of the flow which is quoted by the manufacturers.

One aspect of the gain versus gas flow characteristics is worth noting. In figure 3 the highest gain point plotted for each mixture is that beyond which breakdown occurs. There is a clear maximum in the limiting gain of nearly 3000 at $x = 75\%$. If one combines this optimum with the optimum in the gain versus anode-width curve (figure 4) it proves possible to achieve stable gains of 10 000. Since this gas mixture (argon + 75% isobutane) is very suitable for detecting x-rays of a few keV, it makes a particularly good operating regime.

7. Gain Dependence on Ambient Conditions

The avalanche gain in a gas is strongly dependent on the electron mean free path. Assuming that the electrons behave as a gas this depends on the variable P/T ($= q$) where P is the gas pressure and T its absolute temperature. In a flowing gas situation P follows the atmospheric ambient so that the gain becomes q -dependent. It has been shown elsewhere [11] that allowing the parameter B in equation (2) to take the form $B = aq + b$, where a and b are constants provides an accurate description of the gain behaviour of proportional counters in the pressure/temperature regime around ambient. And that a simple linear servo of the cathode potential can stabilise against this variation.

Figure 9 shows the gain of the $2\mu\text{m}$ anode section of the GMSD over a one week period plotted as a function of q . Fitting an exponential curve to the data automatically gives $1/M dM/dq$ and this evaluates to -0.28K/mB . (P is measured in mB and T in degrees K.) In laboratory conditions the mean value of q is around 3.3mB/K . Assuming that T is roughly constant at around 20C and allowing for maximum excursion of $\pm 50\text{mB}$ this would result in a maximum excursion of $\pm 4.6\%$. A more realistic pressure excursion during an experimental exposure is $\pm 5\text{mB}$ giving a gain shift of $\pm 0.46\%$.

As shown in reference [11] $1/M dM/dq$ does rise slightly with M but tends to stabilise above $M = 1000$. Similarly it is found that it increases with the anode dimension [11] showing a value of around -1.0K/mB for a $10\mu\text{m}$ anode detector at $M \approx 1000$.

8. Total Gain Stability

The data presented in figure 9 demonstrate the total stability of this GMSD over a period of one week. Without any compensation for the variations in q the RMS error in the gain is 0.79% during a period in which ambient pressure changed by 18.5mB . The standard error to the fit in figure 9 shows that this error would be reduced to 0.5% if the calibration data were used to servo V_c to compensate for the changes in q . This residual error level shows that the gas mixing system is delivering at least a stability of 0.1% of the flow over this period. As well as the gas mixing system, the stability of the cathode EHT supply becomes significant at this level and (for applying the q corrections) the precision of the temperature measurement (0.1C) and the lag between the sensor and gas temperature contribute to the residual errors.

In conclusion one can expect GMSD detectors equipped with a good gas mixing system to exhibit short to medium term (RMS) gain stability better than 1% with the potential to achieve 0.5% if a simple EHT servo (which can be implemented automatically or manually) is used to compensate for changes in ambient conditions.

9. Pulse Height (Energy) Resolution

The best relative pulse height resolution (FWHM/peak height) is remarkably constant for all types of proportional counters, being determined by the statistics of the initial electron cloud and the statistical fluctuations in the avalanche process. For the standard gas mixture and 5.9keV x-rays this is $\approx 14.5\%$ and in the few keV x-ray energy region this is found to vary as $(E_{\text{x-ray}})^{-1/2}$ as expected from Poisson statistics. Two factors can degrade the optimum resolution: attachment (and therefore loss to the avalanche process) of drifting electrons and variations in the paths followed by the primary electrons into the avalanche region. Figure 10 shows these two effects at work.

At low drift fields (figure 10) the primary electrons have time to be trapped on electronegative impurities and lost to the pulse causing a position dependence in the output pulse and a spreading of the peak. Thus the relative FWHM decreases sharply as the drift potential is increased until the losses are negligible. As the drift potential is increased there is a weak tendency for the relative FWHM to rise again. This is attributed to the diversion of the primary electrons generated in certain regions of the

drift space into paths close to the cathode which experience higher average fields and thus higher gains, so increasing the FWHM.

As already noted there are good reasons to favour the use of very narrow anode strips. However, figure 10 gives a counter-indication for the narrowest strips which show consistently higher resolutions than the wider ones. Since the worst effect is confined to $w < 4\mu\text{m}$ it is possible to conclude that the optimum anode width (balancing the gain advantages against the pulse height resolution) lies at $w = 4\mu\text{m}$.

10. Application of a GMSD to Electron Yield XAFS.

One attractive application of the GMSD in SRS experiments is for the study of the XAFS (X-ray Absorption Fine Structure) spectra of surfaces using the auger electrons emitted from the surface. This has the advantage over the use of the fluorescent x-ray emission of originating very much closer to the surface than the x-ray emission. The flexibility of the GMSD is demonstrated in the ease with which a demountable sample holder can be built into a simple counter box without compromising any features of the GMSD performance. Figure 11 shows the arrangement of the GMSD plate, the x-ray beam and the sample within the gas enclosure. Melinex windows permitted beam entry (and exit for bragg-scattered beam).

A flow rate of 450cc/min of helium +10% isobutane was used. EHT potentials of $V_c = -750\text{V}$ and $V_d = -2000\text{V}$ gave a gas gain of 1200. The S-8900 plate used had $10\mu\text{m}$ anodes in all sections made in the Ni/Au process by VTT Electronics. Instrumenting each 6mm wide section independently with preamplifier, amplifier, discriminator and scaler enables a global counting rate superior to 1MHz to be achieved.

By minimising the volume of the counter box and maintaining a high gas flow it was possible to change a sample and be acquiring data again within 60 minutes. Provided the plate surface is not touched or scratched, it is simply cleaned by means of a gas puffer and being reflective, is easily checked by eye for dust particles before closing up again.

Figure 12 shows the pulse height spectra obtained in a scan of the x-ray beam energy across the K shell edge of a nickel surface. The characteristic energy spectra of the escaping electrons are seen: below the K edge (8.213keV) the photoelectrons from L and M shells are seen and above the K edge (8.385keV) the addition of the K shell augers is clearly visible. The auger electron spectrum predicted by a simple montecarlo model is shown for comparison. It is noticeable that detection of the incident beam has been very effectively suppressed by the use of the low Z (i.e. mostly helium) gas mixture.

Figure 13 shows the XAFS scans produced by the counts recorded in four of the counter sections which faced the beam footprint on the sample. Analysis of this data demonstrated interesting physics/chemistry which is difficult to access in any other way.

11. Conclusions

From the results of extensive investigations and testing in SRS applications it is concluded that the GMSD offers a unique combination of properties which invite application in internal and external counting experiments in SR (and also in the use of laboratory x-ray generators). These properties may be briefly summarised as follows:

- High counting rate capability
- Adequate gain to detect sub-keV x-rays if necessary
- Stable and uniform gain over large areas and long periods
- Great geometric flexibility as regards the drift region
- Flexible gas mixtures
- Robust and easily cleaned

ACKNOWLEDGEMENTS

We are indebted to Professor T. Rayment of the Chemistry Department, Cambridge University for permission to use figures 11, 12 and 13. We would also like to thank Dr G H Grayer of RAL for his assistance in measuring the plate patterns on the SEM.

REFERENCES

1. A Oed, Nucl Instr & Meth A263 (1988) 351-359
2. F Angelini, R Bellazini, A Brez, M M Massai, G Spandre, and M R Torquati, Nucl Instr & Meth A283 (1989) 755
3. F Angelini, R Bellazini, A Brez, M M Massai, G Spandre, M R Torquati, R Bouclier, J Gauden and F Sauli, IEEE trans Nucl Sci NS-37 (2) (1990) 112
4. F Hartjes, B Hendriksen and F Udo, Nucl Instr & Meth A289 (1990) 384
5. R Bouclier, J J Florent, J Gauden, A Pasta, L Ropelewski, F Sauli and L I Shekhtman, Nucl Instr & Meth A323 (1992) 240
6. R Bouclier G Million, L Ropelewski, F Sauli, Yu N Pestov and L I Shekhtman, Nucl Instr & Meth A332 (1993) 100
7. J E Bateman, J F Connolly, R Stephenson, M Edwards, and J C Thompson, Nucl Instr & Meth A348 (1994) 372
8. R Bouclier, M Capeans, G Manzin, G Million, L Ropelewski, F Sauli, L I Shekhtman, T Temmel, G Della Mea, G Maggioni and V Rigato, CERN Report, CERN-PPE/95-37

9. J E Bateman, J F Connolly, Yu N Pestov, L I Shekhtman, R Mutikainen and I Suni, Rutherford Appleton Laboratory Report, RAL-94-114
10. J J Florent, J Gauden, L Ropelewski and F Sauli, CERN Report, CERN-PPE/92-78
11. J E Bateman, Rutherford Appleton Laboratory Report, RAL-TR-1998-044
12. J E Bateman and J F Connolly, Rutherford Appleton Laboratory Report, RAL-93-090
13. V Peskov, B D Ramsey and P Fonte, Nucl Instr & Meth A392 (1997) 89

FIGURE CAPTIONS

1. A section of the structure of a Gas Microstrip Detector (GMSD). This structure is housed in a suitable gas-tight enclosure.
2. A characteristic plot of the cathode potential, V_c required to keep the gain of a GMSD constant as the drift potential, V_d is increased. The slope of this curve is α in equation (1).
3. A series of gain versus bias curves for a GMSD with 10 μ m wide anodes in a range of argon-isobutane gas mixtures.
4. A plot of the gain of GMSD sections as a function of the width of the anode strip. All other significant parameters are held constant, both mask parameters and operating conditions. Also shown is the curve of the maximum stable gain achieved by each section as a function of the anode width.
5. A plot of the parameter α (equation (1)) as a function of the inverse drift section width (D) for four sections with different anode widths.
6. A plot of the α parameter (equation (1)) as a function of anode width with the drift section width (D) held constant at 11mm. The error bars give the uncertainty given by the fitting process in figure 5.
7. A plot of the gain of two sections of the GMSD with different anode widths as a function of the drift section gap at a constant cathode potential (V_c) of -630V and a drift potential of -2000V. The formulation is derived from the analysis of the data shown in the previous graphs.
8. A plot of the relative sensitivity of the gain ($1/M dM/dx$) to the fraction (by volume) of isobutane in a mixture with argon (x).

9. This shows the gain of a section (2 μ m anodes) of the GMSD measured over a period of one week plotted as a function of the ambient parameter ($q = P/T$ mB/K).
10. The relative pulse height (energy) resolution measured for 5.9keV x-rays in GMSD sections with different anode widths is plotted against the drift potential (V_d). The FWHM is measured as a percentage of the peak pulse height.
11. A schematic drawing of the arrangement of the sample and GMSD plate in the detector used for electron yield XAFS studies.
12. The pulse height spectra observed in a section of the electron yield detector when a nickel sample was irradiated with an x-ray beam with energies just below and just above the nickel K edge.
13. The normalised (to the ion chamber signal) counts seen at each energy in each of four sections of the GMSD during an energy scan of the nickel sample.

FIGURE 1

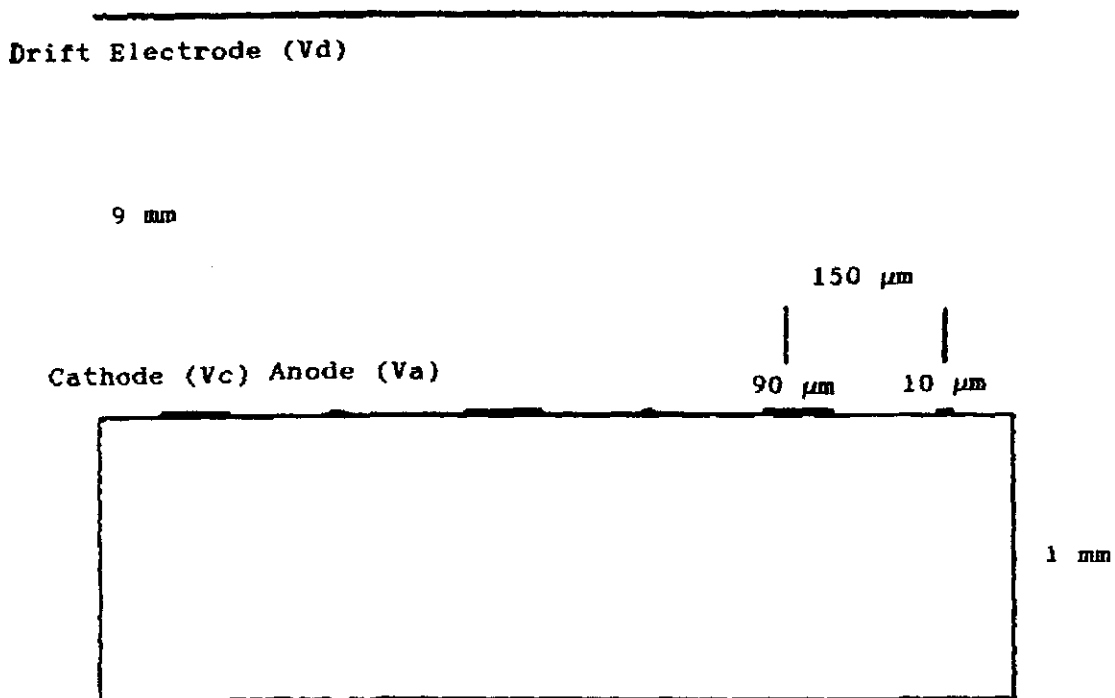


FIGURE 2

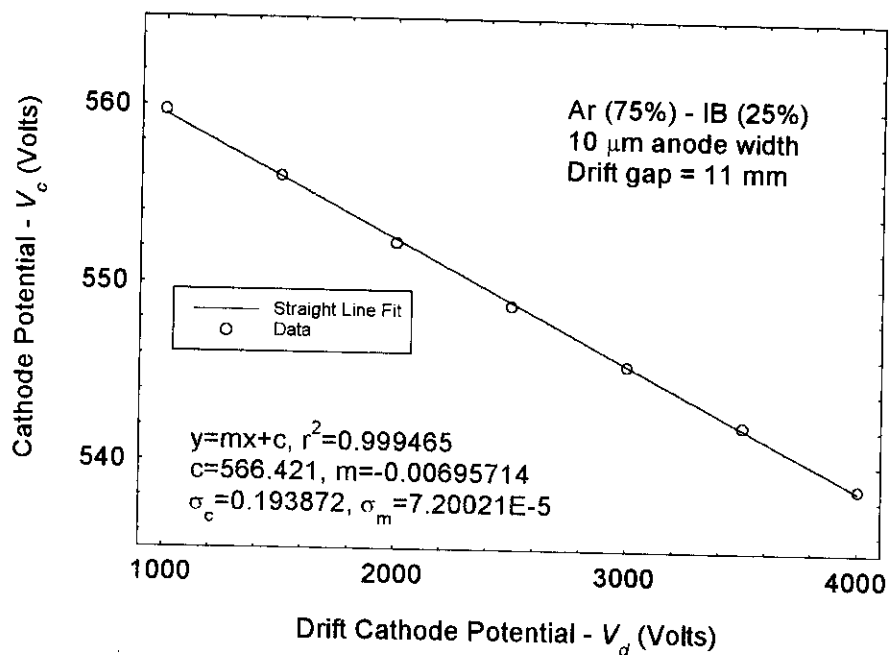


FIGURE 3

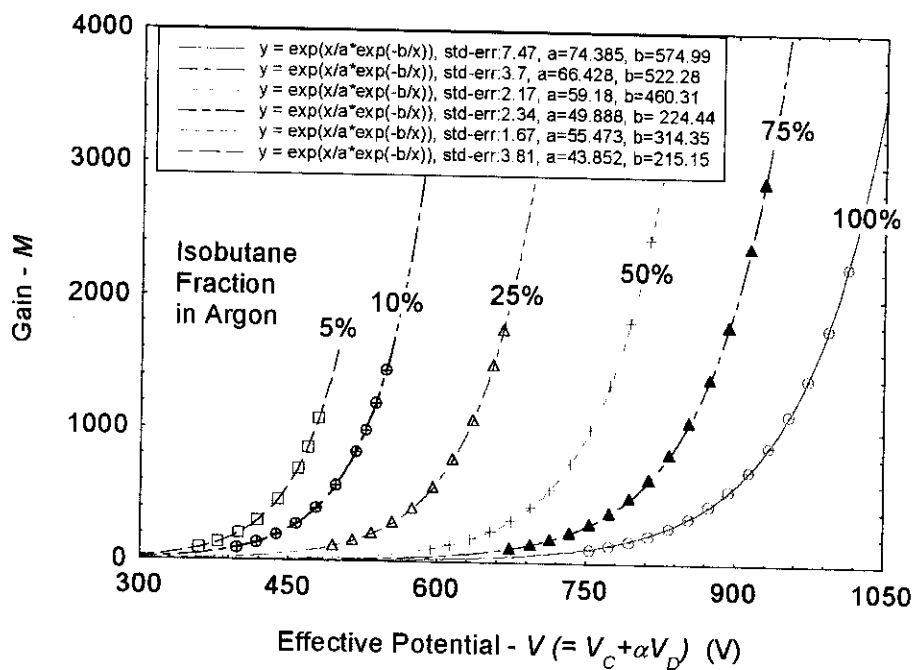


FIGURE 4

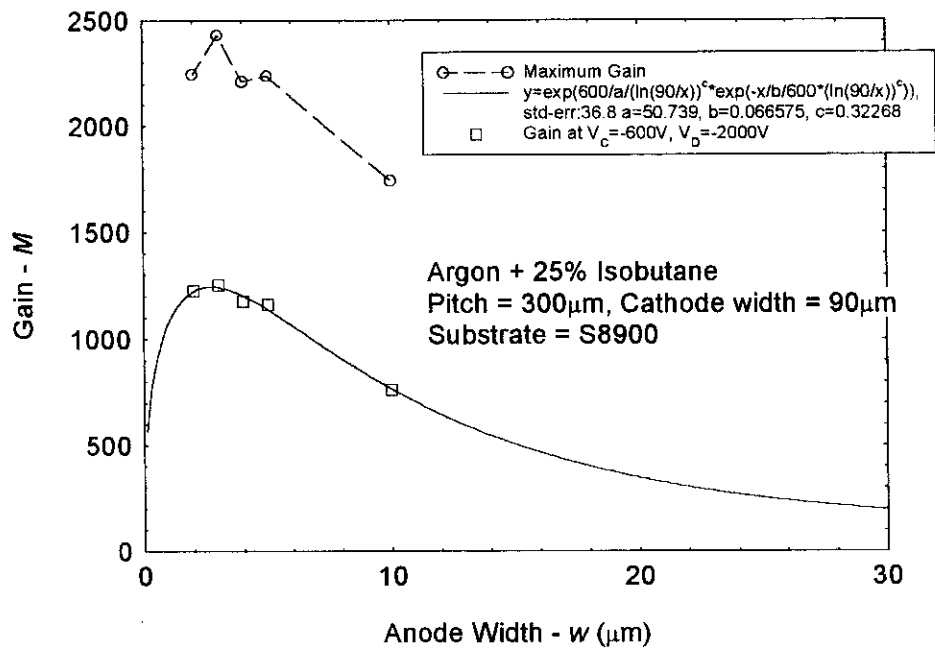


FIGURE 5

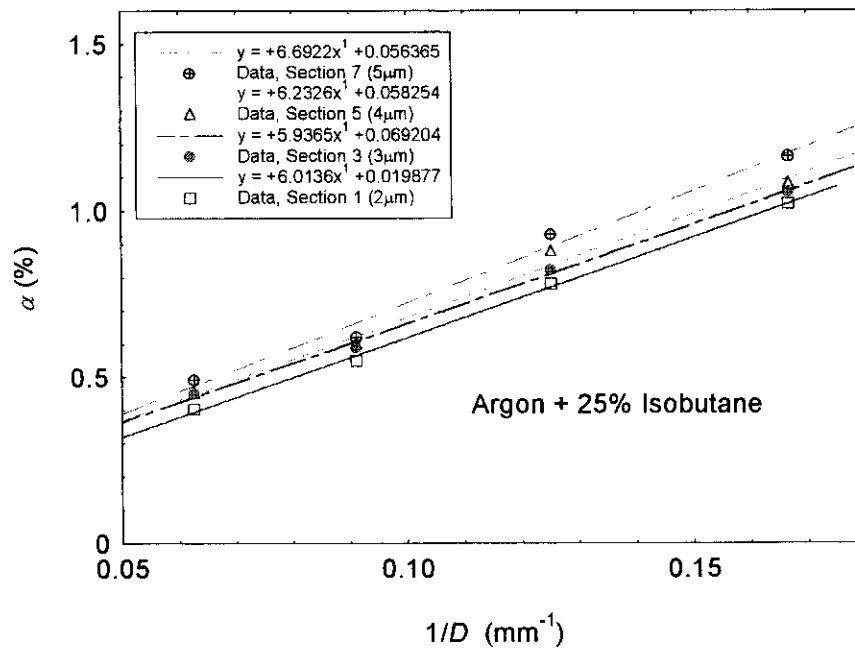


FIGURE 6

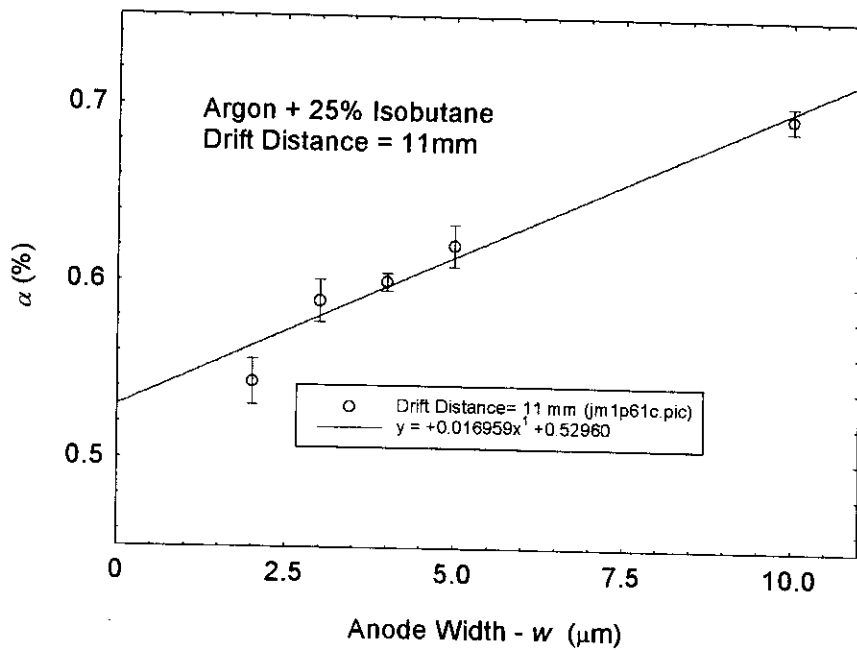


FIGURE 7

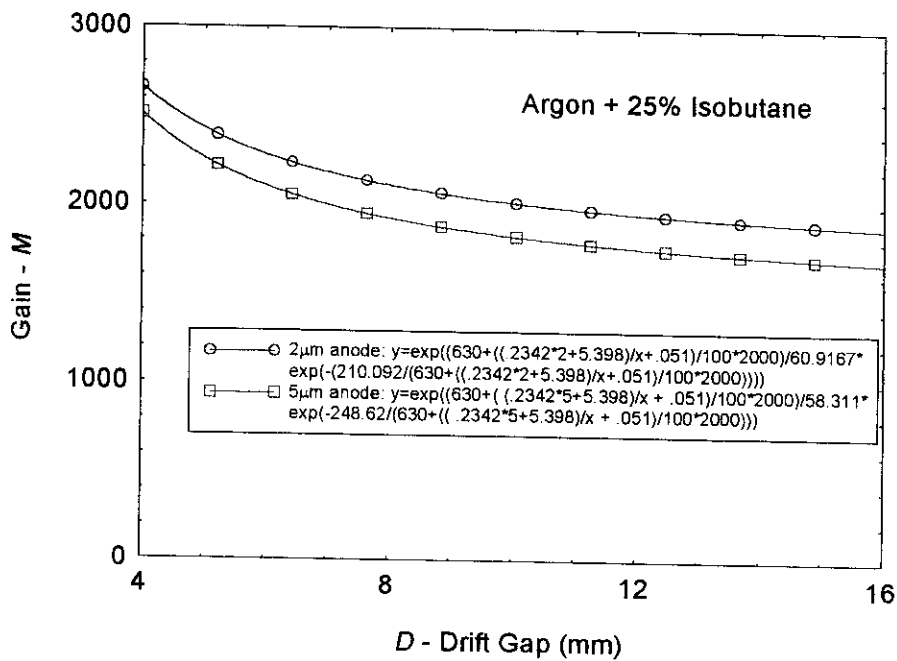


FIGURE 8

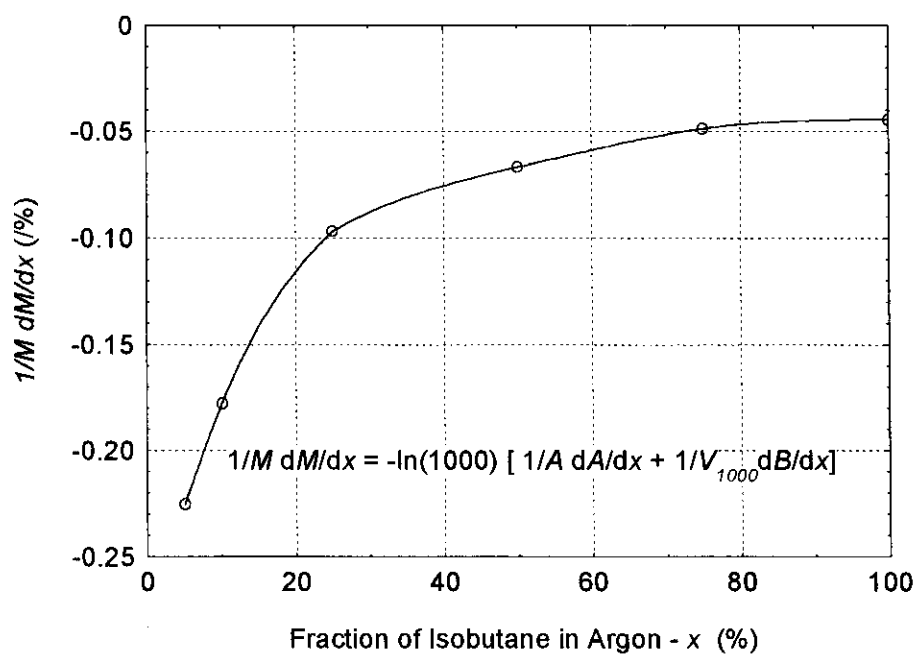


FIGURE 9

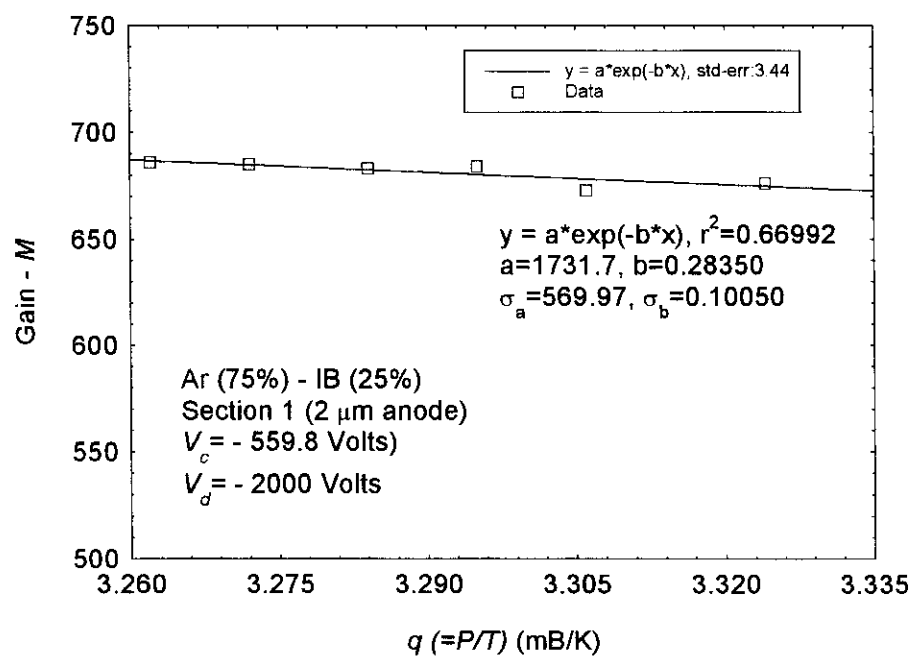


FIGURE 10

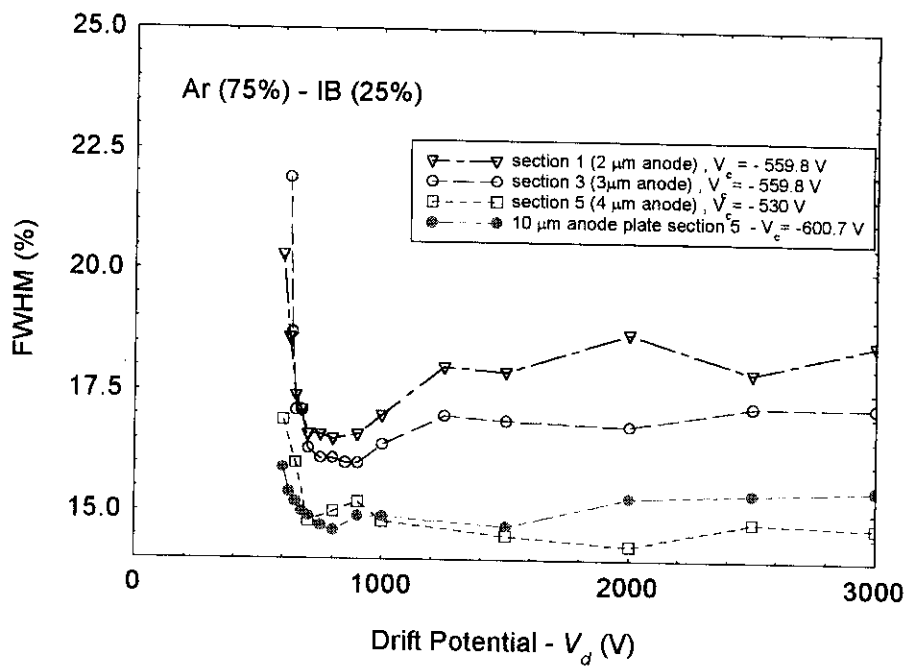


FIGURE 11

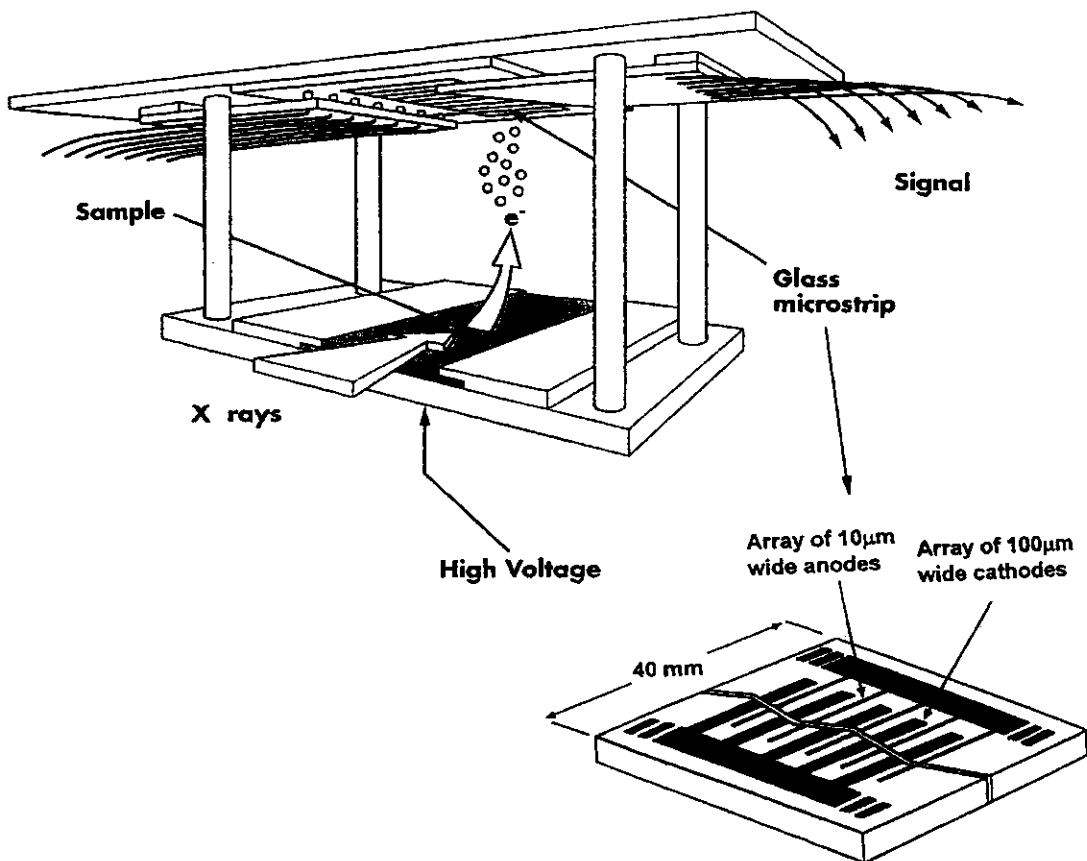


FIGURE 12

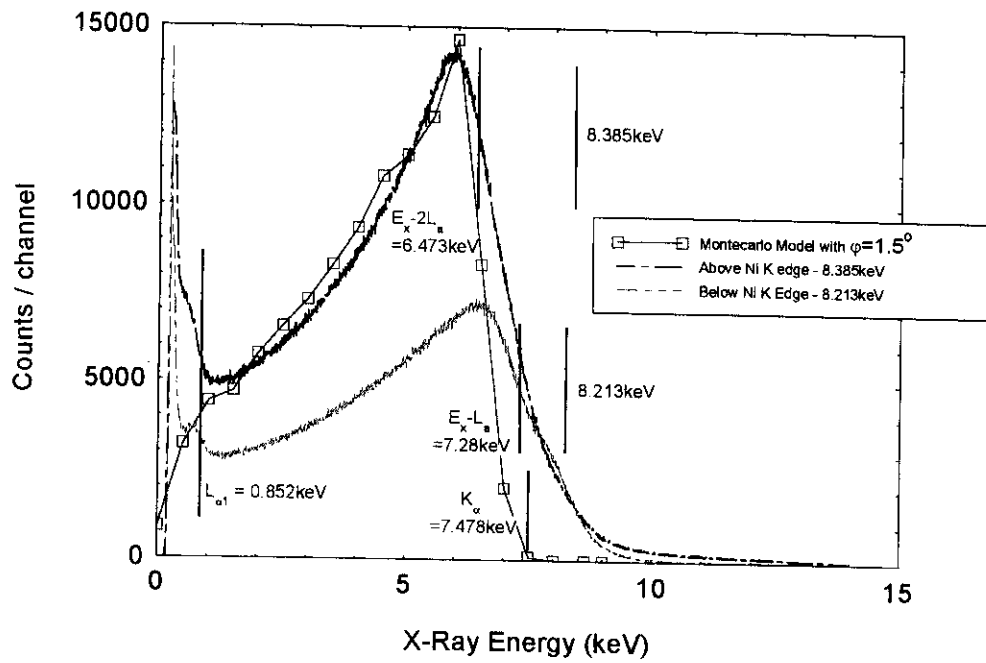


FIGURE 13

